Chapter 12

Realization of Le Rolland-Sorin's Double Pendulum and Some Experimental Results[1]

12.1. Introduction

Among elasticimeters working in the low frequency range, the double pendulum presented here is the simplest instrument to fabricate and to use. Its utilization does not necessitate complicated instrumentation. Only the simplest apparatus are required for measurement.[2] Details of the fabrication of the apparatus are discussed in this chapter and, finally, some experimental results serve to illustrate its versatility.

12.2. Principal mechanical parts of the double pendulum system

The system breaks down into four parts: a frame supporting the sample, jaws for sample clampings at both ends, a platform for the two oscillating pendulums, and the sample itself.

The presentation made here is, to our knowledge, only one possible solution, which is not unique. Readers need only retain the main guiding ideas to conceive

---

Chapter written by Mostefa ARCHI and Jean-Baptiste CASIMIR

1 Long extracts were taken for this chapter from M. Archi's PhD. thesis, Elastic moduli of composite materials by Le Rolland-Sorin's double pendulum, in French [ARC 86]. Dr. Casimir [CAS 10] contributed to the final version of the chapter.

2 The theory of the pendulum can be found in Chapter 8 [CHE 10].

Mechanical Characterization of Materials and Wave Dispersion: Instrumentation and Experiment Interpretation
Edited by Yvon Chevalier and Jean Tuong Vinh

and realize different versions of the instrument and to imagine original apparatus themselves, different to what we present here.

The main idea we wish to underline is the following:

The sample environment, including the sample holder, must have the highest mechanical stiffness with respect to the sample stiffness.

The apparatus and the sample holder must be rigid and have a great mass, and great bending and torsional inertias so that they do not influence the motion of the pendulums and the sample's motion itself.

12.2.1. *Mechanical frame*

Figure 12.1 shows three vertical steel columns which are rigidly fixed to a heavy stand. The high stiffness of the frame in both bending and torsion is obtained by forcing the three vertical columns into three recessed holes in a steel parallelepipedic steel block at the top. Clearance at the top and the contact between columns and the stand are excluded. The columns are assumed to be clamped at the extremities.

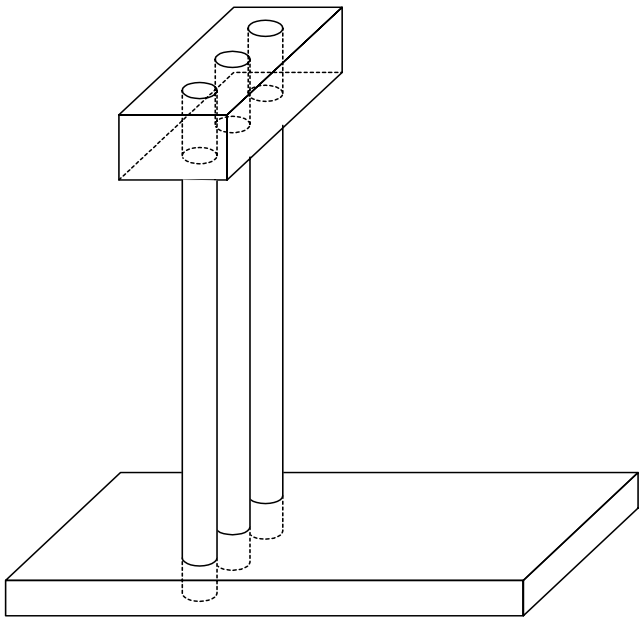

Figure 12.1. *The frame's high bending and torsion stiffness are obtained by three vertical columns rigidly attached together at both ends. The stand hasa heavy weight compared to the set (sample-platform)*

12.2.2. *Jaws for realizing sample clamping*

12.2.2.1. *Pair of jaws to attach the sample to the columns*

A pair of jaws form two adjustable pseudo-clamping positions at the two tips of the sample. Parts A and B (Figure 12.2) have cylindrical grooves which are in contact with the three vertical columns in Figure 12.1. Bolts and nuts (which are not represented in Figure 12.2(a)), help to maintain the jaws firmly in position. A thick steel block with three grooves (Figure 12.2; A and B) serves to fix the jaw, by two bolts, at the desired height depending on the vertical sample length.

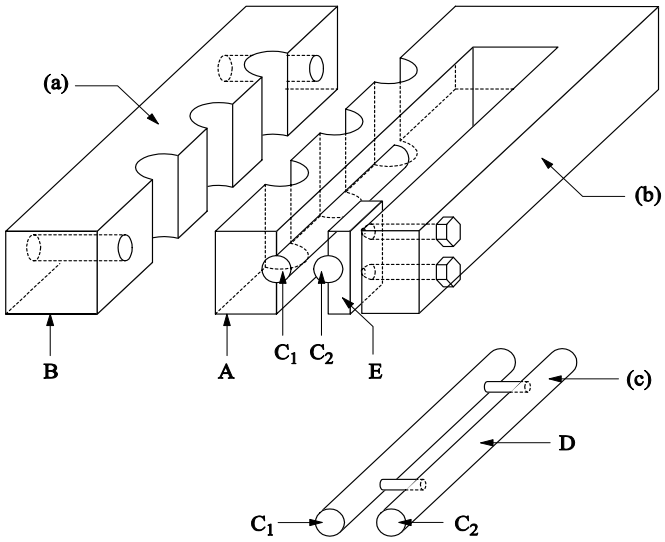

Figure 12.2. *Massive jaws are solidly attached to vertical columns (see Figure 12.1). Parts A and B have cylindrical grooves. Cylinders C_1 and C_2 are parts of the sample pseudo-clamping system. C_1 is fixed in cylindrical grooves in Part A by nuts and bolts. C_2 is connected to C_1 by two guiding cylindrical pins, (Part D in Figure 12.2(c)) so as to ensure the parallelism of the two cylinders. The thick plate E serves to uniformly transmit the compressive force, created by two bolts, to the sample between cylinders C_1 and C_2*

12.2.2.2. *Sample pseudo-clamping by double cylinder system*

Clamping by cylinder is adopted here, and requires sample length correction.[3]

In Figure 12.2(b) the left horizontal cylinder C_1 is an integral part of the jaw in a semi-cylinder groove of part A. The right horizontal cylinder C_2 can be adjusted in its horizontal position with respect to the left cylinder. The parallelism of the two

3 See Chapter 3, section 3.2, which presents the mechanical parts of the vibration test bench.

axes is obtained by means of two guiding cylindrical pins (Figure 12.2(c)). To apply compressive force to the sample along the clamping line, a moving plate E with horizontal groove (Figure 12.2(b)) is used in conjunction with two horizontal bolts whose axes are disposed in a vertical plane at the middle of the sample width.

The distance between the rod axis and the axis of the nearest column must be sufficient to allow the easy attachment of the central platform (which is not represented in Figure 12.2). This precaution is taken when choosing an inertial effect parameter u_1 (equation [10.1]) shaped jaw (Figure 12.2(b)).

12.2.3. *Clamping cylinders*

The two clamping cylinders must be made of hardened steel to reduce the surface deformation during clamping and their eventual permanent plastic deformation; see Figure 12.2(c).

12.2.4. *Platform supporting the two pendulums in the middle of the sample*

Only half of the symmetric platform is represented in Figure 12.3. The platform is a thick plate (a) which is soldered to a thick square vertical rigid bar (b). This last plate is attached to the sample by nuts and bolts. The rectangular open hole on the right (d) serves to install the pendulums in position to create the torsion motion of the sample, which will be explained later.

Figure 12.4 shows a general view of the mechanical system without the pendulums. Cylinder (c) serves to reinforce the rigidity of the horizontal platform (d).

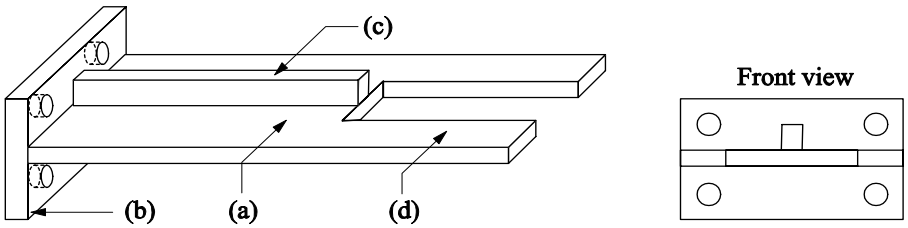

Figure 12.3. *Only half of the platform supporting the pendulum is represented. Its bending stiffness is reinforced partly by means of the T-shaped cross-section of the platform. At the right end, there is a rectangular slot which serves to force torsional sample oscillations by positioning the knife edges of both pendulums appropriately on the platform, with respect to the sample*

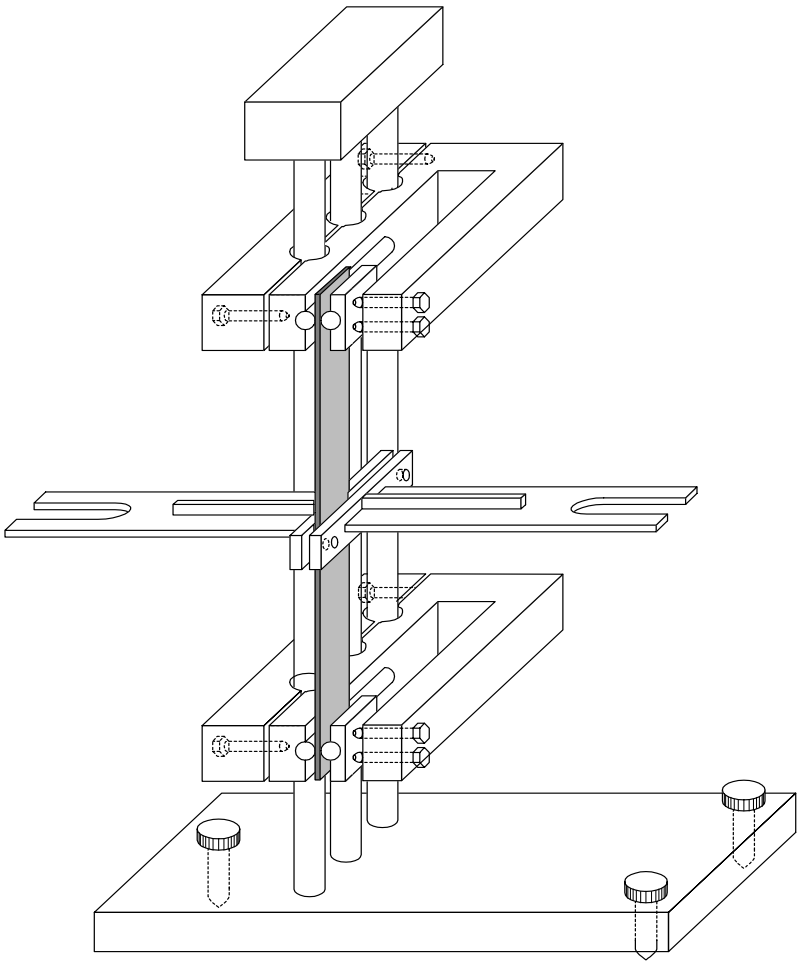

Figure 12.4. *General view of the mechanical system. The horizontal position of the stand is realized by three bolts and nuts with spirit air level. The shape of the central platform is conceived in such a manner that the apparatus can work either in bending test or in torsion test. Pendulums are not represented*

12.2.5. *Pendulums*

The design of each pendulum is made so that it is nearly assimilated to a simple pendulum (meaning that a concentrated mass is oscillating at a distance from the oscillating center). Figure 12.5 shows the components of the pendulum.

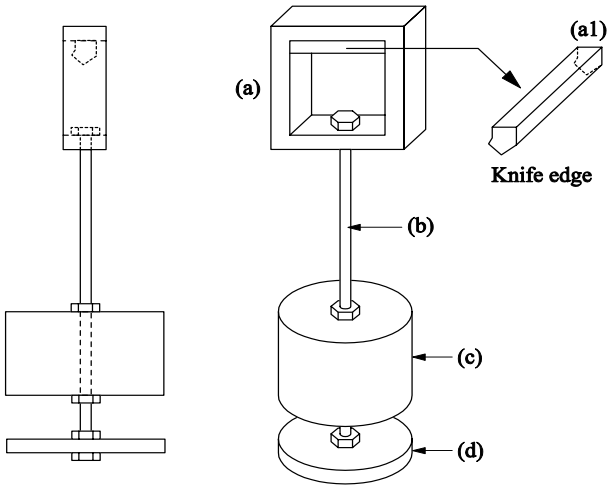

Figure 12.5. *The pendulum is composed of (a) a square frame, which bears a knife edge (presented in detail in (a1)); (b) a cylindrical rod; (c) a massive cylinder weight whose position is adjustable; (d) a complementary weight in the form of a thick disk serving to adjust the pendulum period by changing its position along the rod (b)*

12.2.5.1. *The pendulum and the system-supporting knife edge*

The first part of the pendulum is a square frame made of four steel pieces, see Figure 12.5. The top of the frame is constituted by the knife edge itself (a) which is realized in hardened steel. The square frame is designed to allow pendulums to function either in a bending test or a torsion test. The pendulum is designed to behave like a simple pendulum, i.e. its mass is concentrated at one point along the pendulum's length. For this purpose, a massive cylinder, (c), is fixed to the frame by means of a cylindrical rod; a disk, (d), permits the adjustment of the two pendulum eigenperiods to the same value by varying the disk position with respect to the cylinder (c).

Figure 12.6(b) represents the position of the knife edge with respect to the plate form. Figure 12.6(a) shows the position of both pendulums adopted for a bending test with respect to a sample in a vertical position. Figure 12.6(c) shows that oscillations of both pendulums are in the plane of the figure. Details of the position of the knife edge (BB') are presented in Figure 12.6(b). It is fixed along a cylinder rod which is partly threaded to allow adjustment of the disk position.

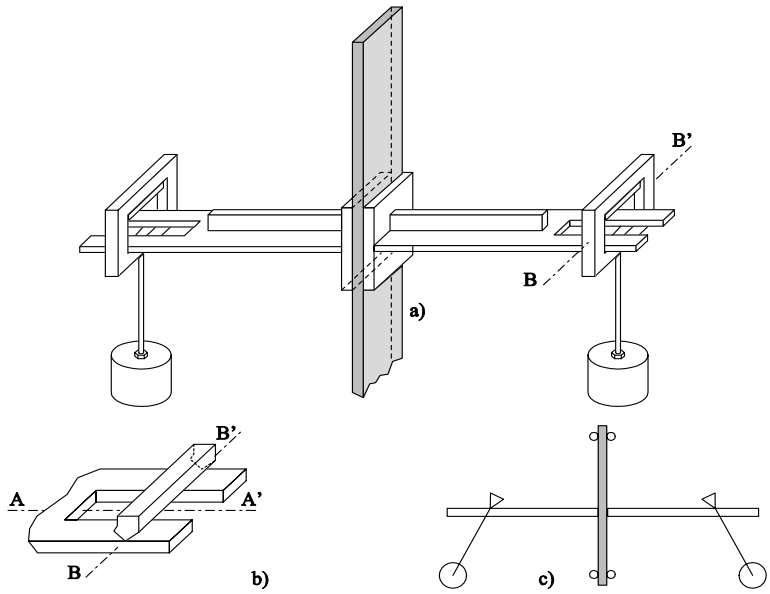

Figure 12.6. *Bending oscillation of the sample: (a) position of the two pendulums at rest; (b) details of the knife edges in the direction BB' are perpendicular to the horizontal axis of the platform. AA'; (c) schematic representation of both pendulums which oscillate in the figure plane*

12.2.5.2. *Pendulum period adjustment*

To facilitate the adjustment of the equality of periods of both pendulums (which constitutes the necessary condition for the good functioning of the apparatus), a disk is disposed under the massive cylinder (d) in Figure 12.5 and serves to adjust the equality of the oscillating period of both pendulums. This operation is effected without the sample on a motionless platform.

12.2.6. *Pendulum positioning*

The position of the pendulum depends on the kind of vibration one wishes to obtain: whether bending or torsional vibration of the sample.

12.2.6.1. *For sample bending*

Figure 12.6 shows the knife edge positioning. The two pendulums oscillate in the plane of the figure i.e. the plane defined by the vertical rod axis and the horizontal symmetry axis of the platform. Figure 12.6(b) shows the position of the knife.

12.2.6.2. *For sample torsion*

Figure 12.7 shows the position of the knife, which is perpendicular to the figure plane. A glass plate is used for this purpose. The knife edge is parallel to the horizontal axis AA' of the platform. A glass plate is used to minimize the friction with the knife edge. The pendulums oscillate in a plane which is perpendicular to the figure.

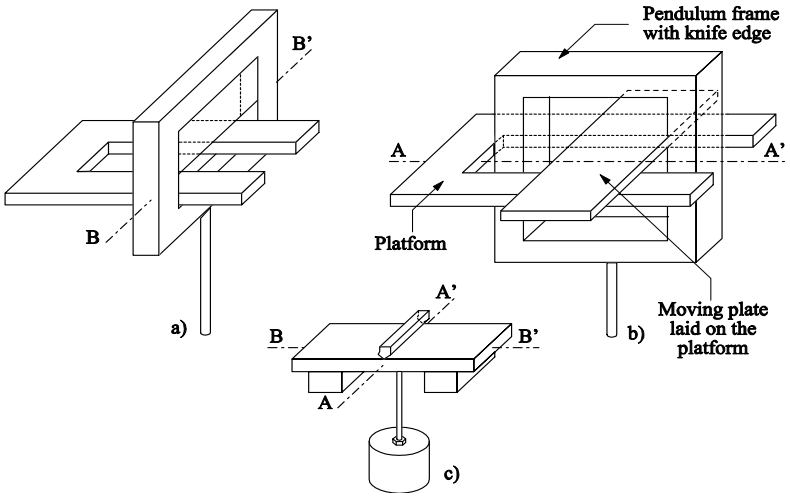

Figure 12.7. *Torsional sample oscillation: (a) for comparison, sample bending vibration is obtained by pendulum oscillations in the figure plane with knife edge contact along the BB' axis; (b) the open slot in half of the platform permits the pendulum knife edge to be positioned in the slot. The knife edge is in contact with a moving rectangular glass plate disposed along the axis AA', perpendicular to axis BB'; (c) position of the knife edge parallel to the sample axis AA'*

12.3. Instrumentation

The instrumentation required is very simple:

– a double pendulum does not necessitate the need for an exciter. The two pendulums contribute alternatively to store and restitute energy via the sample. Free oscillations of both pendulums, for low and medium damping materials, might last a dozen minutes or more;

– the time duration measurement requires either a hand activated chronometer or an electronic chronometer with appropriate electronic gate circuits;

– for damping ratio measurement, electronic recording is necessary.

A displacement transducer is a necessary part of the electronic set-up to record and evaluate beating periods and decreasing amplitude oscillations of one of the pendulums, from which measurement of a logarithmic decrement is evaluated.

Figures 12.8 and 12.9 show respectively that, the sample being in the same position, for a bending test, the pendulums oscillate in the plane (z, x), while for a torsion test, the pendulums oscillate in the plane (z, y). The interest is that, for both tests, the sample is in exactly the same position without modification of the central platform. A change of test nature requires only the change of the direction of the knife edges. For the torsion test, one only has to introduce the glass plate; see Figures 12.7 and 12.9.

Figure 12.10 is a schematic representation of the electronic and electrical set-up. The choice of displacement transducer is large (see Chapter 3). A couple of contactless inductive transducers, even with a low carrier frequency generator to supply the dynamic Wheatstone bridge or eddy current transducer, can be chosen.

Beware the possible non-linear response curve of the transducers. Preliminary calibration is necessary to ensure the linear response. If this is not done, a linearization circuit is necessary. Displacement measurements are taken on one of the pendulums.

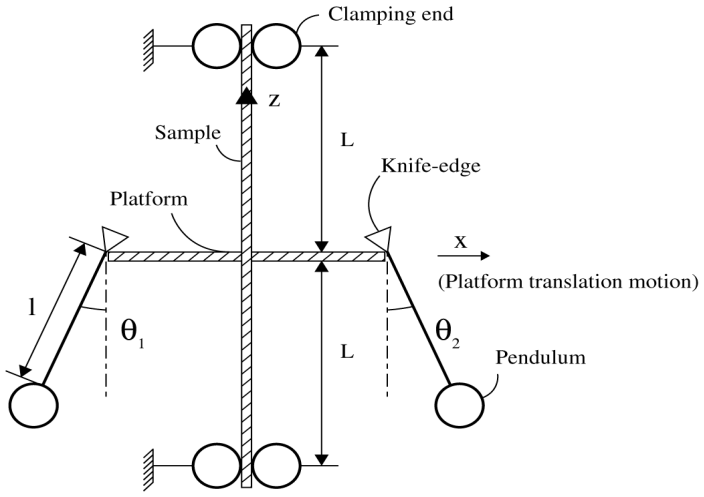

Figure 12.8. *Schematic diagram of the double pendulums showing bending motion of the sample clamped at both ends. The pendulums oscillate in the plane (z,x). 2 L_p is the length of the platform where z is the rod axis and x the direction of the sample thickness*

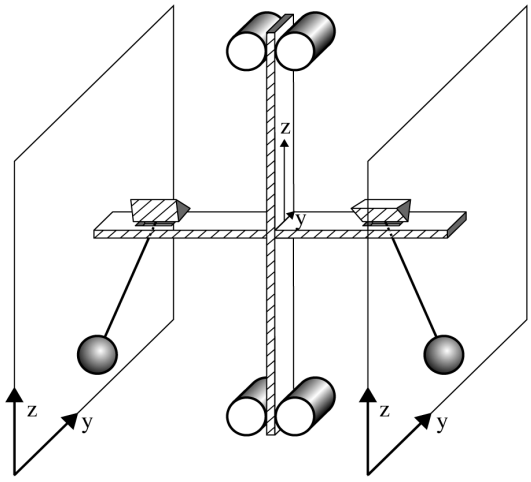

Figure 12.9. *Schematic diagram of torsional double pendulum. The pendulums oscillate in the plane (z,y), where z is the sample axis and y the direction of the sample width*

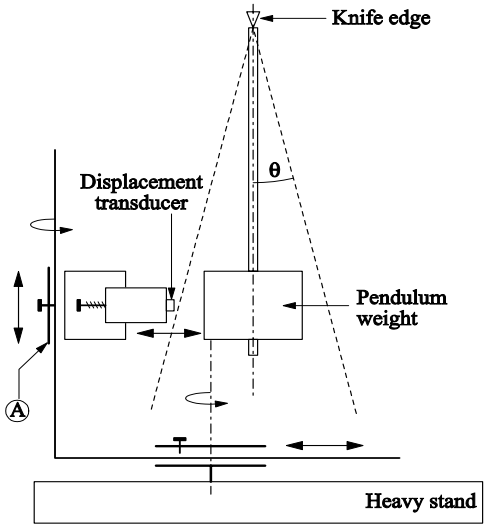

Figure 12.10. *Schematic representation of the electronic set-up. Pendulums need not have large angle oscillations. The recorder is necessary for damping ratio estimation by logarithmic decrement. A couple of transducers working in a push-pull system are used to improve linearity response. Transducers are mounted on guiding bars with adjustable vertical and horizontal positions; (A) is an adjustable guide rail supporting the transducer*

In the case where the elastic (Young's and shear) moduli are the only desired measurements, only a hand-actuated chronometer is necessary, on the condition that the measured beating period of the pendulum exceeds many minutes. For a high damping material, an electronic chronometer is, naturally, adopted.

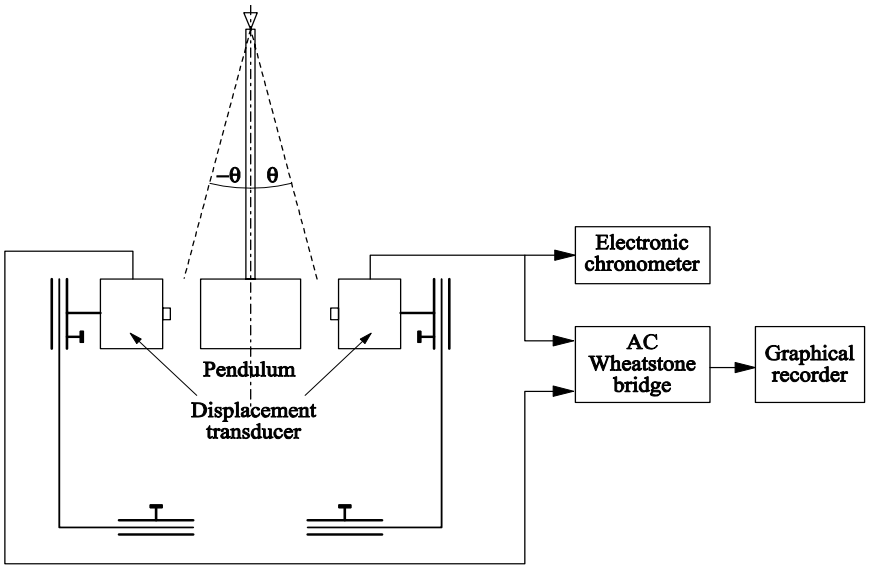

Figure 12.11. *Schematic representation of electronic set-up. It is not necessary to obtain a large oscillation amplitude for the pendulums. Recording of oscillations is necessary for the evaluation of the sample damping coefficient by logarithmic decrement. A couple of contactless transducers working in a push-pull system are used to improve the linearity of the transducers. The transducers are mounted on guiding bars with adjustable vertical and horizontal positions*

12.4. Experimental precautions

The following practical recommendations contribute to obtaining acceptable measurements.

12.4.1. *Platform installation*

The symmetric double platform must be adjusted to the exact middle of the sample. An error in the positioning of the platform clamping with respect to the sample creates a dissymmetry in the oscillations and their amplitude minimum departs from zero.

12.4.2. *Natural oscillation period of the pendulums*

Preliminary adjustment of the natural period of oscillation of each pendulum is necessary. The two oscillation periods of the pendulums must be identical and adjusted separately. Eventually, adjustment of the position of the lower disc permits the period equalization. This is the main precaution to take to obtain further accurate measurements of beating periods with a sample in action. In this case, motion of one of the pendulums gives rise to beating oscillations going to zero amplitude. This precaution enables accurate measurement of beating periods.

12.4.3. *Platform attachment to the sample*

The clamping of the vertical sample to the platform uses classical sample clamping between flat plates so as to avoid possible sample slipping with respect to the platform, taking into account the platform weight. A sample length correction is necessary. The clamping force applied to the two parts of the platform is the important parameter to take into account. For this purpose, the applied force is evaluated via screw tightening by a torque dynamometer key. The torques applied to all the bolts must be equal to ensure the equal distribution of pressure. The curves representing the square of the period versus the sample length, as presented in Chapter 3 (Figures 3.4 and 3.5) enable the evaluation of length correction. This operation requires changes of length of the sample.

12.4.4. *Calibration of displacement transducers*

This calibration corresponds to a given position of the transducers, with the pendulums being at rest. The gaps between transducers and the pendulums are adjusted by means of a key (in the form of steel plates with a predetermined thickness, with an accuracy of 1/100 of millimeter). This operation is followed by electronic calibration of the signal conditioners.

12.4.5. *Geometry of the sample*

This is an important parameter. A preliminary length measurement of the sample is necessary. It should be mentioned that, for bending sample motion, the thickness intervenes as the cube power in the inertia moment. For some multilayered composite samples, the accuracy of the thickness strongly depends on the fabrication of the material itself. This accuracy is rarely lower than 0.1 mm, which is a problem to be accounted for.

12.4.6. *Stability of the stand*

The horizontal position of the stand is a condition of good measurements. The double pendulum system must be sheltered from any parasitic vibrations in the laboratory.

12.4.7. *Electronic triggering circuit for period pendulum measurements*

For a low modulus (soft) material, the beating period can be of the order of several seconds. A hand-activated chronometer lacks accuracy in this condition and can be replaced by an electronic chronometer. An electronic triggering circuit with photodiodes can be used to advantage.

12.4.8. *Damping ratio measurements*

The logarithmic decrement method presented in Chapter 8 in [CHE 10] is the most appropriate one to use to measure the damping ratio. The decreasing of the envelope (which is the mathematical locus) of the maximum pendulum oscillations concerns the beating periods of two combined sinusoidal oscillations. An electronic recorder is then necessary for this purpose; see Appendix 12A.

12.5. Details and characteristics of the elasticimeter

12.5.1. *Characteristics of the double pendulum*

The characteristics below are given only to illustrate the various steps involved in the calculations. Evidently, another set of characteristics will be found with a different pendulum design. Our pendulum characteristics are:

Mass of the two platforms, $m_p = 2.588$ kg

Mass of each pendulum, m = 1. 240 kg

Platform inertia in bending, $I_p = 0.0081$ kg.m^2

Inertia of the platform and the pendulums (torsion tests), $I_p + 2ml^2 = 0.0314$ kg.m^2

Natural periods of each pendulum $T_1 = 0.68$ s

Natural pendulum frequency, $f_1 = 1 / T_1 = 1.47$Hz.

12.5.2. *Elastic modulus calculation programs*

Formulae giving elastic moduli (Young's and shear) are presented in Appendix 12B for both bending vibration and torsional vibration. Non-diagonal compliance matrix coefficients are evaluated for anisotropic materials by using off-axis samples. Appendix 12C presents succinctly the mathematical formulation of the simultaneous bending and torsion of the sample.

12.6. Some experimental results

Details of the fabrication of the pendulums as well as precautions to adjust the mechanical system (clamping of the platform on the sample and its influence on the length correction of the sample, periods of the two pendulums to be equalized etc.) are presented elsewhere (see Chapter 8 [CHE 10]). In this section, we will show that, despite its simplicity of operation, Le Rolland-Sorin's double pendulum can be advantageously compared to more sophisticated instruments.

12.6.1. *Measurements on isotropic metallic materials*

These measurements are used at first to test the reliability of the apparatus.

12.6.1.1. *Aluminum sample*

Thickness h = 2 mm, width b = 15.5 mm; length 2L = 187 mm.

a) Beating period τ_E= 53.27 s (for Young's modulus using bending oscillation);

b) Beating period τ_G = 12.34 s (for shear modulus using torsional vibration).

Measurements on the double pendulum were completed with measurements on ultrasonic benches. Formulae concerning elastic moduli of isotropic materials are the simplest. Details of the successive steps of the calculations are given in [CHE 10] Chapter 8, Figure 8.6. The accuracy of Young's modulus using bending tests depends on the accuracy obtained on the geometry of the sample, essentially on the sample thickness.

For torsion tests, the calculation of shear modulus is given by equations [12.B.5] and [12.B.7] in Appendix 12B. For isotropic material using Saint Venant's theory of torsion, the torsional stiffness is given by (see [12.B.7]) :

$$C_T = bh^3 G\, \beta_T\, (1/c)$$

where c = h/b, with b (width) and h (thickness). β(c) is given by a series formulae in Appendix 12B.

The ultrasonic method permits the evaluation of the stiffness matrix of a material and not the compliance matrix. Consequently, Young's modulus is deduced from C_{ii} and C_{ij} (with $i \neq j$) by matrix inversion. Naturally, the sample is supposed to be essentially elastic and the damping coefficient related to the Young's modulus is supposed to be very low $\tan \delta_E \approx 10^{-2}$.

Table 12.1 gives values of E and G for aluminum, using two different measurement methods.

Elastic modulus	Ultrasonic measurements	Double pendulum measurements
Young's modulus E	5739 x 10^7 Pa.*	5598 x 10^7Pa.
Shear modulus G	2152 x 10^7 Pa.	2110 x 10^7 Pa.

Table 12.1. *Measurement of aluminum with two different methods: ultrasonic and double pendulum.(*). This is not a direct measurement. The Young's modulus is obtained by inversion of the complete stiffness matrix*

12.6.1.2. *Measurement of steel*

Table 12.2 concerns steel elastic moduli.

Beating period	First test	Second test	Third test	Elastic moduli
τ_E	52.4 s.	52.61 s.	52.32 s.	E= 21843 x 10^7 Pa.
τ_G	10.78 s.	10.96 s.	10.83 s.	G=7512 x 10^7 Pa.

Table 12.2. *Measurements with double pendulum for steel*

12.6.1.3. *Measurements of glassfiber–epoxy resin composite (transverse isotropic)*

Length 2L = 186.4 mm; thickness h = 3.4 mm; width b = 10mm; rod axis z = 3

Beating period	First test	Second test	Third test	Elastic moduli
τ_{E3}	64.2 s.	64.10 s.	64.70 s.	E_3= 41.41 x 10^9 Pa.
τ_{G13}	8.50 s.	8.55 s.	8.44 s.	G_{13}= 5.1 x 10^9 Pa.

Table 12.3. *Measurements of a glass epoxy composite $G_{13}=G_{23}$; plane (1,2) is transversely isotropic. τ_{E3}= beating period in bending vibration; τ_{G13}= beating period in torsional vibration*

12.6.1.4. *Glass epoxy composite*

This material is transverse-isotropic. The rod axis, z, is perpendicular to the fiber axis 3 (Figure 12.9).

Length 2L = 113mm; width b= 10.7 mm; thickness h= 3.45 mm; density ρ = 1946 kg/m^3

Beating period	First test	Second test	Third test	Elastic moduli
τ_{E1}	74.35 s.	74.23 s.	74.60 s.	E_1=9.58 x 10^9 Pa.
τ_{G12}	15.48 s.	15.47 s.	15.38 s.	G_{12}= 5.27 x 10^9 Pa.

Table 12.4. *Measurements of glass fiber-epoxy resin composite. Rod axis is along direction 2, perpendicular to fiber axis 3*

12.6.2. *Non-diagonal compliance coefficient of anisotropic material*

Details of the mathematical formulation of simultaneous bending and torsion of an off-axis sample are presented elsewhere (see Chapter 8 [CHE 10]). Here, we give some remarks on the testing method and its accuracy.

The main problem to be solved is the coupling between bending and torsion due to the utilization of an off-axis sample. As the rod axis z is not coincident with the reference material axis, compliance matrix coefficients must be calculated for the sample reference axis. The compliance matrix being of the fourth order, a change of reference axes gives rise to the power four of the direction cosines in the formulae (see Chapter 1 in [CHE 10]).

This constitutes the main problem in compliance coefficient calculation. To take this into account in practice, optimization calculation methods are referred to. An

example of the calculation of Poisson's number for boron fiber-epoxy resin is presented below.

12.6.2.1. *Preliminary measurement of compliance matrix coefficient, the axis of the material being coincident with the sample axis*

In a first step, the matrix diagonal coefficients must be evaluated before envisaging the non-diagonal matrix coefficient calculations. In this preliminary calculation stage, a sample whose reference axes coincide with the reference material axes is used.

Two samples are necessary, one sample with fiber axis 3 perpendicular to the rod axis z, as in Figure 12.12. The other sample has its z axis coinciding with fiber axis 3.

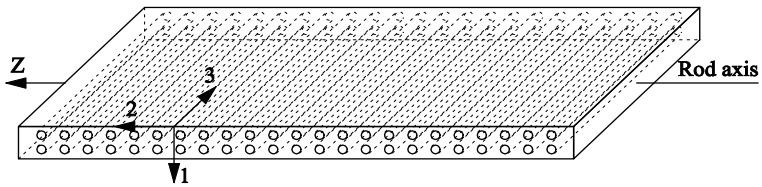

Figure 12.12. *Rod axis z with respect to fiber axis 3*

Two elastic moduli are obtained for each sample:

a) $E_1 = 24.5 \times 10^9$ Pa. $G_{13} = 2.25 \times 10^9$ Pa.

b) $E_3 = 204.6 \times 10^9$ Pa. $G_{12} = 2.25 \times 10^9$ Pa.

12.6.2.2. *Calculation of Poisson's ratio* ν_{13}

Figure 12.13 presents the variation of $\nu_{31} = \nu_{31}$[4] versus the shear modulus G_{13} and the rotation angle α between fiber axis and rod axis. The sensitivity of ν_{13} with respect to shear modulus G_{13} is less pronounced than that with respect to angle α. The calculation program gives the compliance component of boron fiber epoxy resin composite: $s_{13} = -1.47 \times 10^{-12}$ Pa^{-1}.

4 This equality means the material is transverse isotropic and has a symmetric axis 3

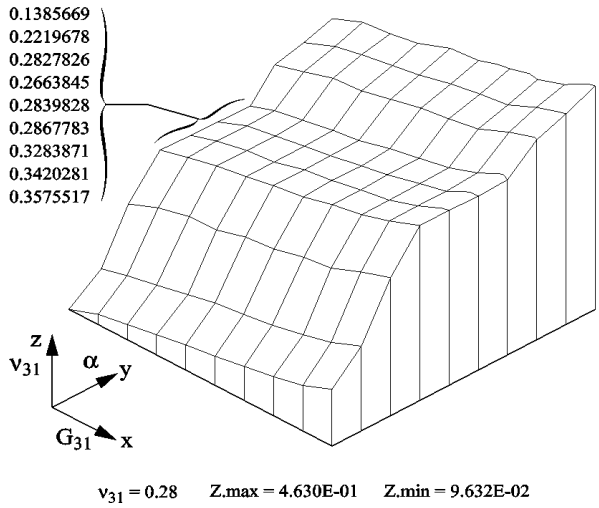

Figure 12.13. *Variation of Poisson's number ν_{31} versus shear modulus G_{13} and the angle α between fiber axis and rod axis z. Optimization method consists in finding the stationary zone*

The corresponding Poisson's number is: $\nu_{13} = -s_{13}E_3 = 0.28$

Details of calculation of s_{35} and ν_{31} with formulae can be found in [CHE 10] Chapter 8, Appendix 8D.

12.7. Damping ratio estimation by logarithmic decrement method

This method is presented and discussed, with possible improvements by special signal processing (see Chapter 8 regarding the time Hilbert transform). With the double pendulum, two records of beating oscillations are presented in Figure 12.14. Only a few beating periods are presented in this figure. The beating angular frequency is represented by the difference ($\omega_1 - \omega_2^*$); ω_2^* with the star designating the complex natural angular frequency of the viscoelastic sample, which concerns the envelope of the pendulum 1 oscillations. ω_1 is the natural angular frequency of the pendulum, which is supposed to be real. The position of one point on the envelope at an instant t depends on the value $(\omega_1 - \omega_2^{'})$t and also on ω_1t. Calculation of the logarithmic decrement can be effected.

The mathematical expression of oscillation is:

$$\theta_1(t) = \theta_0(0)\, e^{-\omega_2^{''}t}[\cos(\omega_1 - \omega_2^{'})\frac{t}{2}]. \cos\omega_1 t \qquad [12.1]$$

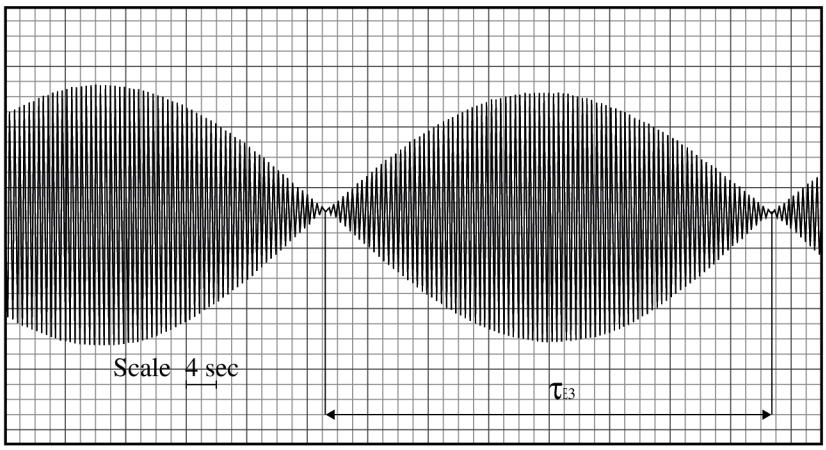

Figure 12.14. *Record of pendulum (1) oscillations. The pendulum is launched at its maximum amplitude with zero initial velocity $\theta_1'(0) = 0$. τ is the beating period. The material damping coefficient is evaluated from the envelope of oscillations*

where: ω_1 is the natural circular frequency of the pendulum 1;

ω_2' is the real part of natural complex circular frequency of the sample;

ω_2'' is the imaginary part of the sample circular eigenfrequency.

After [12.1] the beating period is given by:

$$(\omega_1 - \omega_2')\frac{\tau}{2} = k\pi \text{ , k integer} \qquad [12.2]$$

where k is an integer.

$$\tau = \frac{2k\pi}{\omega_1 - \omega_2'} \qquad [12.3]$$

The choice of amplitudes of pendulum 1 is such that the time interval must be:

$$t_{measured} = n\,\tau \qquad [12.4]$$

where n is a positive integer. If the time translation is effected with reference to the initial amplitude A_0^p, the other amplitude on the other beating period is A_0^p or A_2^p, etc.

Relation [12.4] must be satisfied. The damping ratio is related to the slope of a graphical curve of the envelope of a graphical curve of the envelope in a semi-logarithmic coordinate: $\zeta_2 = -$ slope / $(\omega_1 - \omega_2')$.

And the damping ratio is expressed as ln, designating a Naeperian (or natural) logarithm:

$$\zeta_2 = \frac{1}{n} \ln \left[\frac{A_0^p}{A_n^p} \right] \qquad [12.5]$$

The translation of time such that A_0^0 is replaced by A_0^p, and p is the integer number of the natural period of pendulum (1). A_n^p designates the amplitude, with n being the rank of beating period and p the notation indicated above.

The material damping is defined as the ratio of the imaginary part to the real part of the viscoelastic modulus:

$$\tan \delta_E = \frac{Im[E^*]}{Re[E^*]} = \zeta_2^E / \pi \qquad [12.6]$$

To take the example of boron-epoxy composite with unidirectional fibers, for Young's modulus E_3^* and shear modulus G_{13}^*:

$$\zeta_E = \frac{1}{7} \ln \frac{151}{129} = 0.0225$$

$$\tan \delta_{E3} = \frac{0.0225}{\pi} = 0.0071$$

$$\zeta_{G13} = \frac{1}{10} \ln \frac{164}{143} = 0.0137$$

$$\tan \delta_{G13} = \frac{0.0137}{\pi} = 0.0044$$

12.8. Concluding remarks

The double pendulum presented in this chapter has absolutely no resemblance to any other industrial elasticimeter. It is based on a completely different functioning principle with respect to classical apparatuses which include two main independent parts: (a) oscillator and exciter, and (b) a set of transducers.

12.8.1. *Absence of external exciter*

Le Rolland-Sorin's pendulum does not need an external exciter. One of the pendulums is launched by gravity and the potential energy due to the initial amplitude of pendulum 1 is sufficient to maintain the oscillations of the two pendulums during the experiment's duration. By exchanging energy, oscillations of each pendulum are maintained with a slow decrease in amplitude. The main features to be remembered are:

– measuring instruments are reduced: a chronometer is sufficient to evaluate elastic moduli;

– additional instruments (transducers and recorders) enable this apparatus to explore the domain of viscoelasticity of materials;

– possible extension of measurements to characterization of composite materials by using an off-axis sample;

– its ease of use;

– it is of interest for working in the lowest working frequency (just a few Hertz).

To work in this frequency range, a hydraulic exciter working in sinusoidal regime requires a great deal of room and apparatus.

12.9. Bibliography

[ABA 72] ABARCAR R.B., CUNIFF F.F., "The vibrations of cantilever beam of fiber reinforced materials", *J. Composite Materials*, vol. 6, pp.504, 1972.

[ARC 87] ARCHI M., Evaluation of elastic constants of composite material by Le Rolland-Sorin's coupled pendulum, PhD thesis, Conservatoire national des Arts et Métiers, Paris, I.S.M.C.M. Saint Ouen, France, in French, 1987.

[CAS 10] CASIMIR J.B., "Measurement of damping coefficients of materials by Le Rolland-Sorin's double pendulum". Forthcoming. 2010.

[CHE 10] CHEVALIER Y., VINH T., *Mechanics of Viscoelastic Materials and Wave Dispersions*, ISTE Ltd, London, and JohnWiley & Sons, New York, USA, pp 425-486, 2010.

[GIE 59]GIET M.A., "On the determination of material elastic constants by forced vibrations", *GAMI Review*, in French, 1959.

[JOH 71] JOHNSON A.F., Bending and torsion of anisotropic beams, Report DNAM, National Physics Laboratory, England, March, 1971.

[KAN 58] KANTOROVICH L.V., KRYLOV V.I., *Approximate Methods of Higher Analysis,* Groninger, Noordhoff, Netherland, 1958.

[KER 68] KERR A., "An extension of Kantorovich method", *Quaterly Applied Mathematics*, July 1968.

[KOL 63] KOLSKY H., *Stress Waves in Solids*, Dover Ed., New York, pp. 132-136, 1963.

[LER 14] LE ROLLAND P., "On the determination of the ratio of oscillation durations of two pendulums", *Comptes rendus Académie des Sciences*, Vol.1, 159, Paris, in French, 1914.

[LER 33] LE ROLLAND P., "Application nouvelle du pendule aux problemes industriels et en particulier au contrôle des matériaux", *Bulletin de la société d'encouragement pour l'industrie nationale*, May 1933, pp. 317-347, (http// : cnum.cnam.fr/pdf/cnum_ BSPI.148.pdf)

[LER 34] LE ROLLAND P., "About a method using coupling between two oscillating systems to evaluate mechanical strength of structures and elastic moduli", *Scientific and Technical Publication of Air Force Ministry*, paper no. 47, 178 pages, in French, 1934.

[LER 48] LE ROLLAND P., "About a new method for the determination of intense solid friction and the energy dissipation", *Comptes rendus Académie des Sciences*, Paris, vol. 227, p.37, in French, 1948.

[NUG 76] NUGUES M., Study of elastostatic torsion of a beam with rectangular cross section – Dynamic torsion of anisotropic beam, thesis, CNAM, Paris, 29th June 1976.

[RIT 75] RITCHIE I.G., ROSINGER H. E., "Torsional rigidity of rectangular section bars of orthotropic materials", *J. Composite Materials*, vol.9, 1975.

12.10. Appendix 12A. Equations of motion for the set (pendulums, platform and sample) and Young's modulus calculation deduced from bending tests

12A.1. *Equations of motion*

Kinetic energy U_c and potential energy of the system are (Figure 12.6 and 12.8]):

$$U_c = \frac{1}{2}\left(m_p \dot{x}^2 + m\left(\dot{x} + L\,\dot{\theta}_1\right)^2 + m\left(\dot{x} + L\,\dot{\theta}_2\right)^2 \right) \qquad [12.A.1a]$$

$$U_p = \frac{1}{2}\left(mg\,L\,\theta_1^2 + mg\,L\,\theta_2^2 + k\,x^2 \right) \qquad [12.A.1b]$$

with m_p being the platform mass, m the pendulum mass, k the sample translation rigidity, g the gravity acceleration, l the length of the pendulum, x the horizontal displacement of the platform, and θ_1 and θ_2 the oscillation amplitudes of the pendulums.

Lagrange's equations are deduced, the dots on the letters designating the time derivative of the corresponding variable

$$\left.\begin{aligned} m_p\left(\ddot{x} + L\ddot{\theta}_1\right) + m\left(\ddot{x} + L\ddot{\theta}_2\right) + k\,x = 0 \\ m\,L\left(\ddot{x} + L\ddot{\theta}_1\right) + L\,mg\,\theta_1 = 0 \\ m\,L\left(\ddot{x} + l\ddot{\theta}_2\right) + L\,mg\,\theta_2 = 0 \end{aligned}\right\} \qquad [12.A.2]$$

$$\left.\begin{aligned} \ddot{x}\left(m_p + 2\,m\right) + \ddot{\theta}_1\,mL + \ddot{\theta}_2\,mL + k\,x = 0 \\ \ddot{x} + L\ddot{\theta}_1 + g\,\theta_1 = 0 \\ \ddot{x} + L\ddot{\theta}_2 + g\,\theta_2 = 0 \end{aligned}\right\} \qquad [12.A.3]$$

The pendulums are supposed to be simple for the first presentation. To obtain a non-trivial solution, the determinant of the coefficients in [12.A.3] is set to zero. This gives the eigenfrequency.

The eigenvalue equation is obtained by setting the determinant of [12.A.3] to zero:

$$\begin{vmatrix} k - \omega^2\left(m_p + 2m\right) & -mL\omega^2 & -mL\omega^2 \\ -\omega^2 & g - L\omega^2 & 0 \\ -\omega^2 & 0 & g - L\omega^2 \end{vmatrix} = 0 \qquad [12.A.4]$$

By developing [12.A.4]:

$$\left[g - l\,\omega^2\right]\left[k - \omega^2\left(m_p + 2m\right) - 2m\,l\,\omega^4\right] = 0 \qquad [12.A.5]$$

A solution corresponds to

$$\omega_1^2 = g/L$$

This gives the eigenfrequency of the pendulums ω_1. The second factor of the developed determinant is:

$$\omega^4 \left(L\, m_p\right) - \omega^2 \left[k\, L + g \left(m_p + 2m\right)\right] + kg = 0 \qquad [12.A.6]$$

The two roots of [12.A.6] are positive.

The greatest root corresponds to motion at highest frequency. This higher mode of vibration tends to disappear rapidly with time. The lowest mode remains and it is easily shown that the corresponding circular frequency is lower than the pendulum eigen circular frequency.

$$\omega_2 < \omega_{pendulum} = \omega_1 \qquad [12.A.7]$$

12A.2. ***Solutions for pendulum oscillations***

The solutions $\theta_1(t)$ and $\theta_2(t)$ depend on the initial conditions adopted for the pendulums:

$$t = 0 \quad \theta_1 = \theta_0 \quad , \quad \dot{\theta}_2 = \quad \theta_2 = \dot{\theta}_1 = \dot{x} = x = 0 \qquad [12.A.8]$$

The platform is initially at rest, as is the second pendulum. Pendulum 1 is launched at $\theta_1 = \theta_0$ and without initial angular velocity: $\dot{\theta}_1 = 0$.

Details of calculations of $\theta_1(t)$ are presented by using the Laplace transform (Chapter 8 [CHE 10]).

Taking into account the practical construction of the pendulums, we have to deal with the coupling of two mechanical oscillators of eigenfrequencies ω_1, ω_2.

As both pendulums are identical and only the first pendulum is launched at amplitude θ_0 without initial velocity, the two pendulums oscillate in phase opposition.

$$\left.\begin{aligned} \theta_1(t) &= \theta_0 \cos\left(\frac{\omega_1 + \omega_2}{2}\right) t.\cos\left(\frac{\omega_1 - \omega_2}{2}\right) t \\ \theta_2(t) &= \theta_0 \sin\left(\frac{\omega_1 + \omega_2}{2}\right) t.\sin\left(\frac{\omega_1 - \omega_2}{2}\right) t \end{aligned}\right\} \qquad [12.A.9]$$

A beating phenomenon of the two oscillators takes place, and in [12.A.9] the envelope of oscillation corresponds to a beating period:

$$\tau = \frac{2\pi}{\omega_1 - \omega_2} \qquad [12.A.10]$$

12A.3. *Relationship between beating period τ and sample stiffness k*

12A.3.1. *Stiffness calculation*

By setting $\omega_1^2 = g/l$ and $\omega_2 = \omega$ the lower circular eigenfrequency is the root of the following equation:

$$\left[k - \omega^2 \left(m_p + 2m\right)\right]\left(g - L\omega^2\right) - 2mL\omega^4 = 0 \qquad [12.A.11]$$

$$k\left(g - L\omega^2\right) = \omega^2\left(m_p + 2m\right)g - \omega^4 m_p L$$

Sample stiffness is deduced:

$$k = \frac{\left(m_p + 2m\right)\omega^2 \frac{g}{L}}{\left(\frac{g}{L} - L\omega^2\right)} - \frac{\omega^4 m_p}{\left(\frac{g}{L} - \omega^2\right)}$$

That gives the sample stiffness when $\omega = \omega_2$

$$k = \frac{\left(m_p + 2m\right)\omega_2^2\,\omega_1^2}{\left(\omega_1^2 - \omega_2^2\right)} - \frac{\omega^4 m_p}{\left(\omega_1^2 - \omega_2^2\right)} \qquad [12.A.12]$$

$$\delta = \frac{T_1}{\tau} = \frac{\omega_1 - \omega_2}{\omega_1} \quad ; \quad \tau = \frac{2\pi}{\omega_1 - \omega_2} \qquad [12.A.13]$$

$$\omega_2 = \omega_1 (1 - \delta) \qquad [12.A.14]$$

Bringing [12.A.13] and [12.A.14] into [12.A.11]:

$$k = \frac{(m_p + 2m)(1 - \delta)^2}{\delta(2 - \delta)} \omega_1^2 - \frac{(1 - \delta)^4}{\delta(2 - \delta)} m_p \omega_1^2 \qquad [12.A.15]$$

or

$$\boxed{k = \omega_1^2 \left[m_p + \frac{2m}{\delta(2 - \delta)} \right] (1 - \delta)^2} \qquad [12.A.16]$$

The sample stiffness k depends on the relative beating period δ in [12.A.16], with m and m_p being the parameters of the pendulum system itself.

12A.4. *Young's modulus calculation*

The Young's modulus is related to the sample stiffness by classical formula used in the strength of material:

$$k = \frac{48 E I}{L^3} \qquad [12.A.17]$$

The sample is clamped at both ends and a platform is attached in its middle. As the platform is associated with the sample without sliding, some precautions are necessary for the fixing of the platform. In later chapters, details are given to take into account the clamping force applied between the platform and the sample. The length of the sample consequently necessitates a correction. In [12.A.17] I is the inertia moment of the sample:

$I = \frac{b h^3}{12}$, where b is the width, and h the thickness.

12.11. Appendix 12B. Evaluation of shear modulus by torsion tests

Equations of motion of Le Rolland-Sorin's double pendulum working in torsion are similar to the equations of motion in bending tests presented in Appendix 12A.

12B.1. *Energy expression*

The potential and kinetic energies are (dots on the letters designate time derivatives):

$$U_p = \frac{1}{2}\left(C\,\theta_p^2 + m\,g\,L\,\theta_1^2 + m\,g\,L\,\theta_2^2\right) \qquad [12.B.1]$$

$$U_c = \frac{1}{2}\left[I_p\,\dot{\theta}_p^2 + m\left(L_p\,\dot{\theta}_p + L\dot{\theta}_1\right)^2 + m\left(L_p\,\dot{\theta}_p + L\,\dot{\theta}_1\right)^2\right]$$

Lagrange's equations of motion are deduced:

$$\begin{aligned} &I_p\ddot{\theta}_p + m(L_p\ddot{\theta}_p + L\ddot{\theta}_1)L_p + m(L_p\ddot{\theta}_p + L\ddot{\theta}_2)L_p + C\theta_p = 0 \\ &m(L_p\ddot{\theta}_p + L\ddot{\theta}_1)L + mgL\theta_1 = 0 \\ &m(L_p\ddot{\theta}_p + L\theta_2)L + mgL\theta_2 = 0 \end{aligned} \qquad [12.B.2]$$

where I_p, L_p and θ_p designate respectively the inertia moment of the platform, the length the torsional angle of the platform

$$C = \frac{2\,C_T}{L} \qquad [12.B.3]$$

where C_T is torsional stiffness.

Arranging [12.B.2] we obtain the following equations:

$$\begin{aligned} \left(I_p + 2\,m\,L_p^2\right)\ddot{\theta}_p + m\,L\,L_p\,\ddot{\theta}_1 + m\,L\,L_p\,\ddot{\theta}_2 + C\,\theta_p &= 0 \\ L_p\,\ddot{\theta}_p + L\,\ddot{\theta}_1 + g\,\dot{\theta}_1 &= 0 \\ L_p\,\ddot{\theta}_p + L\,\ddot{\theta}_2 + g\,\theta_2 &= 0 \end{aligned} \qquad [12.B.4]$$

Comparing [12.B.4] to [12.A.3] we notice that the two sets of equations are similar. The solutions obtained previously for flexural vibrations can be transposed here by changing corresponding coefficients:

$$C = \left[\frac{(1-\delta)^2}{\delta(2-\delta)}\left(I_p + 2\,m\,L_p^2\right) - \frac{(1-\delta)^4\,I_p}{\delta\,(2-\delta)}\right]\omega_1^2$$

$$C = \omega_1^2\,(1-\delta)^2\left[I_p + \frac{2\,m\,L_p^2}{\delta\,(2-\delta)}\right] \qquad [12.B.5]$$

$$C = 2\,\frac{C_T}{L} \qquad [12.B.6]$$

The torsion stiffness of a rod with rectangular cross-section is given by Saint Venant's theory:

$$C_T = b\,h^3\,G_{xz}\,\beta_T\,(1/c) \qquad [12.B.7]$$

where $\beta_T(c)$ is a warping function deduced from Saint Venant's torsion formula:

$$c = \frac{h}{b}\sqrt{\frac{G_{xz}}{G_{yz}}}, \qquad [12.B.8]$$

$$\beta(c) = \left[\frac{1}{3} - \frac{63}{c\pi^5}\sum_{1,3,5}\frac{1}{k^5}\tanh\left(\frac{k\pi c}{2}\right)\right] \qquad [12.B.9]$$

where b is width, h thickness, and G_{yz} and G_{xz} the shear moduli in the planes yz and xz, respectively. In the case of isotropic materials, these two moduli are equal and c is reduced to the ratio of width (b) to thickness (h) in formula [12.B.8].

C is deduced from the measured beating period δ. Torsional stiffness C_T is evaluated from C. Shear modulus is obtained from equation [12.B.7].